

# Exergy analysis of an ethanol fuelled proton exchange membrane (PEM) fuel cell system for automobile applications

Shuqin Song<sup>1</sup>, Savvas Douvartzides, Panagiotis Tsiakaras\*

Department of Mechanical Engineering, School of Engineering, University of Thessaly, Pedion Areos, 383 34 Volos, Greece

Accepted 25 February 2005

Available online 3 May 2005

## Abstract

An integrated ethanol fuelled proton exchange membrane fuel cell (PEMFC) power system was investigated following a second law exergy analysis. The system was assumed to have the typical design for automobile applications and was comprised of a vaporizer/mixer, a steam reformer, a CO-shift reactor, a CO-remover (PROX) reactor, a PEMFC and a burner. The exergy analysis was applied for different PEMFC power and voltage outputs assuming the ethanol steam reforming at about 600 K and the CO-shift reaction at about 400 K. A detailed parametric analysis of the plant is presented and operation guidelines are suggested for effective performance. In every case, the exergy analysis method is proved to allow an accurate allocation of the deficiencies of the subsystems of the plant and serves as a unique tool for essential technical improvements.

© 2005 Elsevier B.V. All rights reserved.

**Keywords:** Exergy; PEM; Ethanol

## 1. Introduction

The utilization of alternative fuels such as ethanol for generation of electrical power in fuel cells may be considered as a long-term policy capable of providing significant economic and environmental benefits [1]. For many governments, ethanol represents a domestic energy source, an answer to the alleged future CO<sub>2</sub> emission taxation and the liquid renewable fuel which rises the least impediments on the conversion of their existed gasoline infrastructures [2–4]. Due to these reasons, ethanol has recently acquired a renewed interest in the fuel cell vehicle community [5–9].

During the last decade, the automobile industry has adopted the technology of the *proton exchange membrane fuel cell* (PEMFC) as the most appropriate for power generation [10,11]. PEMFCs are electrochemical devices able to efficiently generate electricity, operating at low temperatures. Hydrogen is the ideal fuel for PEMFCs, the only chemical species that may be adequately oxidized on the anode electrocatalyst of the cell at the selected operating temperatures (350–400 K). However, a number of obstacles to the production and storage of pure hydrogen, have altogether forced the vehicle industry in the design alternative for onboard hydrogen production from a raw organic fuel, through catalytic processes such as the steam reforming and the CO-shift reaction. This fact resulted in an increase of the complexity of the power system, not only due to the addition of a reformer and a CO-shift reactor but also due to the necessity for the addition of a secondary energy source, a heat producing reactor (a burner) that would sustain the endothermic reaction of the steam reformer. Even further, the inability of the PEMFC catalysts (usually Pt or Pt/C) to tolerate the poisonous CO species from the reformat resulted also in the inevitable addition of one more reactor, aiming at the selec-

*Abbreviations:* DEFC, direct ethanol fuel cell; ED, overall exergy destruction in all devices of the plant; ELH, overall exergy loss through all heat wastes from the plant to environment; EFG, overall exergy loss due to material waste; PEMFC, proton exchange membrane fuel cell; LHV, low heating value of ethanol (=1,235,000 J)

\* Corresponding author. Tel.: +30 24210 74065; fax: +30 24210 74050.

E-mail address: [tsiak@mie.uth.gr](mailto:tsiak@mie.uth.gr) (P. Tsiakaras).

<sup>1</sup> On leave from the Direct Alcohol Fuel Cells Laboratory, Dalian Institute of Chemical Physics, CAS, P.O. Box 110, Dalian 116023, China.

**Nomenclature**

<i>a</i>	number of ethanol moles in the initial mixture with steam
<i>b</i>	number of steam moles in the initial mixture with ethanol
<i>c</i>	number of CO <sub>2</sub> moles in the initial reacting mixture of the CO-shift reactor
<i>d</i>	number of H <sub>2</sub> moles in the initial reacting mixture of the CO-shift reactor
<i>e</i>	exergy (J)
<i>f</i>	number of H <sub>2</sub> O moles in the initial reacting mixture of the CO-shift reactor
<i>g</i>	number of CO moles in the initial reacting mixture of the CO-shift reactor
<i>h</i>	specific enthalpy (J mol <sup>-1</sup> )
<i>h</i>	efficiency of the heat transfer from the burner (%)
<i>l</i>	energy loss from the burner to the environment as a percentage of the LHV of ethanol (%)
<i>m</i>	mass flow rate (kg s <sup>-1</sup> )
<i>p</i>	pressure (bar)
<i>Q</i>	amount of heat (J)
<i>R</i>	universal gas constant (=8.314 J mol <sup>-1</sup> K <sup>-1</sup> )
<i>s</i>	specific entropy (J mol <sup>-1</sup> K <sup>-1</sup> )
<i>T</i>	absolute temperature (K)
<i>V</i>	PEMFC voltage (V)
<i>W</i>	PEMFC power (kW)
<i>x</i>	number of ethanol moles reacting in the steam reformer
<i>x</i>	molar fraction
<i>y</i>	number of H <sub>2</sub> moles reacting in the steam reformer
<i>z</i>	number of CO moles reacting in the CO-shift reactor

*Greek letters*

$\Delta H$	enthalpy difference (J mol <sup>-1</sup> )
$\lambda$	factor of air excess in the PEMFC

*Superscripts*

CH	indicative of the chemical exergy component
CO	indicative of the CO oxidation reaction
<i>e</i>	indicative of a species present in the environmental chemical composition
heat	indicative of exergy flow due to heat flow
H <sub>2</sub>	indicative of the H <sub>2</sub> oxidation reaction
PH	indicative of the physical exergy component
ref	indicative of the reactions occurring in the reformer
shift	indicative of the reaction occurring in the CO-shift reactor
vap	indicative of the ethanol vaporization

*Subscripts*

cr	critical quantity
H	indicative of a thermal sink of high temperature
H <sub>2</sub>	indicative of the H <sub>2</sub> incoming in the PEMFC
H <sub>2</sub> O	indicative of the steam produced in the PEMFC
<i>i</i>	indicative of a specific chemical species or a specific heat flow
O <sub>2</sub>	indicative of the O <sub>2</sub> incoming the PEMFC from air
r	reduced quantity
0	indicative of the standard conditions at 298 K and 1.013 bar
1	indicative of the ethanol steam reforming reaction
2	indicative of the H <sub>2</sub> reaction in the reformer
3	indicative of the CO-shift reaction

tive oxidation of CO (usually referred as the PROX reactor) [10,11].

The increased complexity of these power systems leads to a significant decrease of the overall energy conversion efficiency, far below the values calculated by the thermodynamic studies of the autonomous PEMFC device, and also in requirements for an appropriate energy management. In this direction, first law energy considerations are usually employed, in terms of the amount of energy of each stream of matter and heat inside the system, and results are obtained according to simple energy calculations aiming at the determination of the operation conditions (temperatures of reforming and CO-shift reactions, hydrogen utilization, etc.) that are preferable in practice. Although theoretically sound, these studies are unable to depict the magnitude of perfection of the operation regime of the individual subsystems of the plant. Second law considerations are inevitable when trying to avoid these drawbacks.

The “exergy analysis method” has been established since the age of the postulation of the second law and is capable of defining a measure of quality in the amount of energy, depending on the macroscopic conditions of the state at which this energy quantity is available [12–14]. By using “exergy” as the term for this quality of energy, simple calculations may provide valuable results for the departure of the operation regime of a device or a plant from perfection. By following the entropy generation principle of the second law of thermodynamics and by defining “exergy destruction” (ED) as the product of the entropy generated with the temperature of the environment (the Gouy–Stodola theorem) the exergy analysis provides an allocation of the exergy destruction rate in the individual subsystems of the power plant and a quantification of the order of excellence of the involved processes.

In the last decade, a number of papers dealing with the exergy analysis of proton exchange membrane (PEM) fuel cells fuelled by various fuels were published [15–18]. In

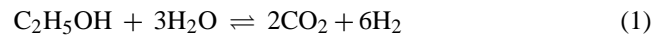
the present study, the exergy analysis method was undertaken to illuminate the role of the second law analysis in the improvement of the theoretical studies of an automobile PEMFC system fuelled by ethanol. The power system was analyzed assuming an ethanol mass flow rate of  $0.046 \text{ kg s}^{-1}$  ( $1 \text{ mol s}^{-1}$ ).

## 2. Model development

### 2.1. Chemical and electrochemical processes

A FORTRAN model was constructed to simulate a proton exchange membrane fuel cell (PEMFC) power plant fuelled by ethanol. The plant (Fig. 1) was assumed to consist of a vaporizer/mixer, a reformer, a CO-shift reactor, a CO-remover (PROX reactor), a PEMFC and a burner. Adjusted gaseous streams of ethanol and steam (with an appropriate steam/ethanol molar ratio RF equal to or greater than the stoichiometric for ethanol reforming) were routed to the reformer. The equilibrium composition of the following simul-

taneous reactions:



was established at a temperature of about 600 K. Both reactions (1) and (2) are endothermic and take place with heat supplied from the burner. Further, the water-gas shift reaction



was assumed to lead in equilibrium at a temperature of about 400 K. Reaction (3) is weakly exothermic and its role is to consume a significant amount of CO in the reformat mixture while producing additional amounts of hydrogen. Given that CO is a potentially poisonous species for the Pt catalysts of the PEMFC, its fraction in the fuel cell feed-stream must be lower than 10 ppm if it causes no obvious effect on PEMFC performance [10,11]. To meet this requirement, the resulting mixture is routed to a CO-remover (PROX) reactor where the selective CO oxidation takes place according to the

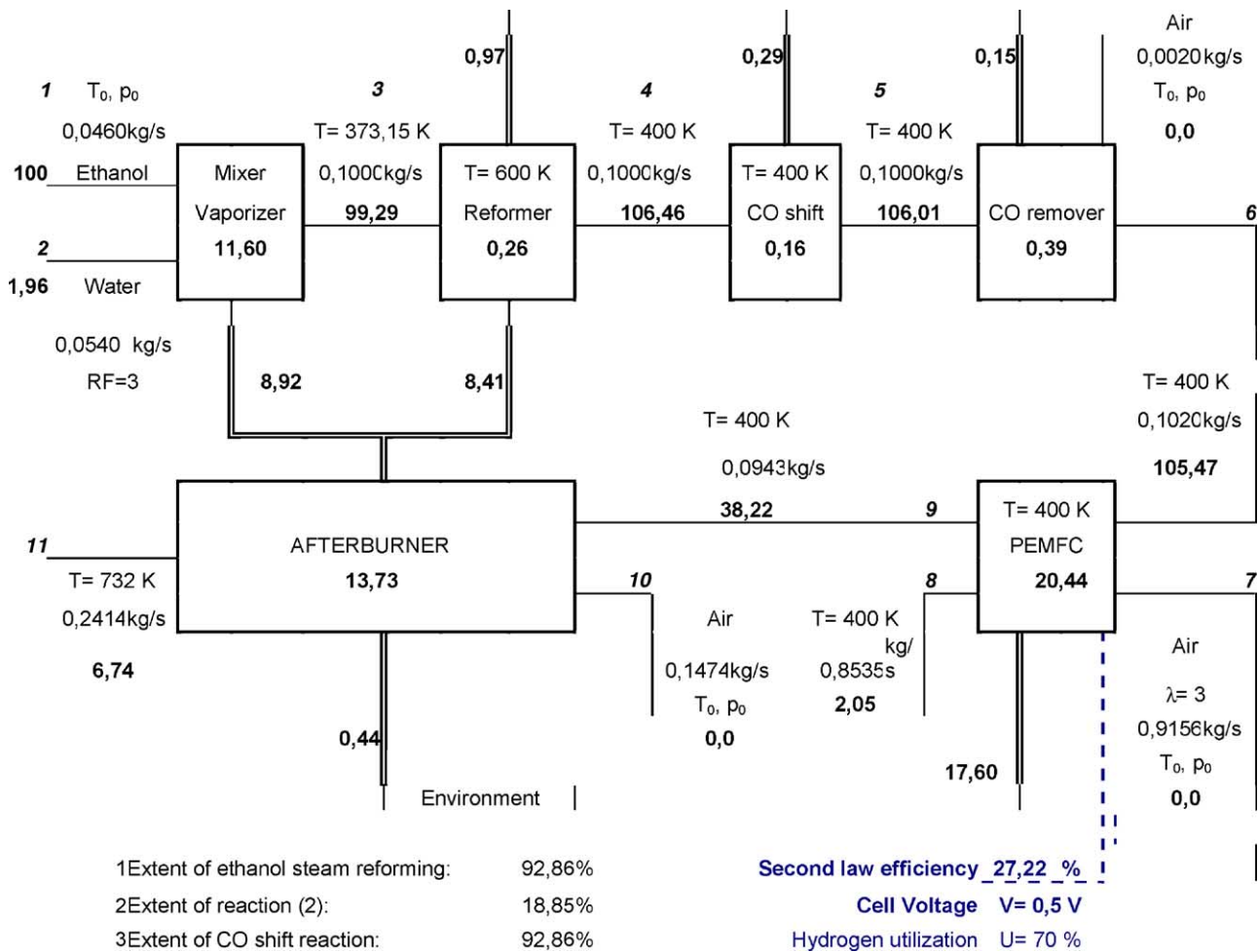


Fig. 1. Analysis of the PEMFC power system for  $T_{\text{ref}} = 600 \text{ K}$ ,  $T_{\text{shift}} = 400 \text{ K}$ ,  $U = 70\%$ ,  $V = 0.5 \text{ V}$ . The total exergy destruction in the plant is 38.22% of the chemical exergy of ethanol and the second law efficiency is 27.22%.

Table 1

The extent (%) of the reaction of ethanol steam reforming as a function of the temperature of the reaction and the selected reforming factor

Temperature of reforming (K)	Equilibrium constant, $K_1$	RF = 3 (stoichiometric)	RF = 4	RF = 5
300	$7.78 \times 10^{-13}$	3.40	3.45	3.52
350	$4.68 \times 10^{-8}$	8.00	9.96	11.85
400	0.00018	21.99	27.30	32.37
450	0.110496	44.92	55.56	65.05
500	18.7839	69.08	84.14	93.73
550	1255.14	85.03	98.25	99.81
600	41633.8	92.86	99.93	99.99
650	805820	96.40	99.99	99.99
700	$1.021 \times 10^7$	98.04	99.99	100.00
750	$9.227 \times 10^7$	98.85	100.00	100.00
800	$6.331 \times 10^8$	99.28	100.00	100.00

exothermic reaction



The air required for reaction (4) was calculated in all cases to be stoichiometric to the amount of CO. Finally, the CO-depleted and hydrogen rich mixture produced by the above series of reactions is routed to the PEMFC anode. Hydrogen is electrochemically dissociated on the anode catalyst into protons, which migrate through the proton exchange membrane to the cathode. The electrons released from the anode reaction are also routed to the cathode through an external circuit and the following electrochemical reduction occurs:



Cathode reaction (5) is exothermic and closes the electron flow mechanism that corresponds to the desired electricity generation from the plant.

In the present study, it should be noted that the proton exchange membrane is not strictly assumed to be the currently commonly used Nafion<sup>®</sup> membrane. Instead, the analysis assumes also PEM fuel cells with other membrane types, which may be still under investigation but can be resistant to higher temperatures. In the case of Nafion<sup>®</sup> membrane in which proton transportation depends on the water content in the membrane, the operation temperature of the PEMFC must be sufficiently low (below 373.15 K) in order to retain the electrolyte hydrated and facilitate the H<sup>+</sup> migration mechanism. For this reason, an appropriate cooling system was tacitly considered for the successful rejection of the heat released by reaction (5). The PEMFC was assumed to operate with a power output  $W$  and an overall voltage  $V$  so that the following relations were used to calculate the mass flow rates of hydrogen consumption ( $\dot{m}_{\text{H}_2}$ ), oxygen demand ( $\dot{m}_{\text{O}_2}$ ) and steam formation ( $\dot{m}_{\text{H}_2\text{O}}$ ) which are all expressed in terms of  $\text{kg s}^{-1}$ :

$$\dot{m}_{\text{H}_2} = 1.05 \times 10^{-8}(W/V) \quad (6)$$

$$\dot{m}_{\text{O}_2} = 4.12 \times 10^{-7}(\lambda W/V) \quad (7)$$

$$\dot{m}_{\text{H}_2\text{O}} = 9.45 \times 10^{-8}(W/V) \quad (8)$$

Eqs. (6)–(8) are corrected forms of the equations given by Larminie and Dicks [19] in order to take into account the exact chemical composition of the atmospheric air which is assumed in the present exergy analysis. Further,  $\lambda$  in Eq. (7) denotes the stoichiometric coefficient of air supply in the PEMFC.

In every case, hydrogen utilization in the PEMFC was adjusted to be appropriate for a positive energy balance of the burner. In many cases, depending on the temperature of the reformer and the selected reforming factor, the amount of ethanol that remains unreformed is not sufficient to supply all heat demands through a direct combustion in the burner. In these cases an appropriate lowering of the hydrogen utilization in the PEMFC is inevitable so that the burner undertakes also the combustion of a certain amount of hydrogen. The combustion conditions in the burner were always considered stoichiometric.

Vaporization of water and ethanol was assumed to take place in the vaporizer/mixer at 373.15 K and 1.013 bar. In other words, for each kilogram of steam production in the vaporizer a heat demand of 2676.1 kJ was taken into account ( $48169.8 \text{ J mol}^{-1}$  of steam). On the other hand, given that ethanol vaporization occurs below 373.15 K, a standard correlation method was used according to Majer and Svodoba [20] for the calculation of the enthalpy of gaseous ethanol at 373.15 K. According to this method, at any temperature above the boiling point of ethanol, its enthalpy content may be given by:

$$\Delta H^{\text{vap}} = 50.43 \exp(0.4475T_r)(1 - T_r)^{0.4989} \text{ kJ mol}^{-1} \quad (9)$$

where  $T_r = T/T_{\text{cr}}$  is the reduced temperature with  $T_{\text{cr}} = 513.9 \text{ K}$ .

The calculation of the extent of the reaction (1) was accomplished depending on the temperature and the reforming factor using an iterative convergent method and the results are given in Table 1. Then the calculation of the extents of the reactions (2) and (3) was straightforward following a typical thermodynamic analysis. By knowing the mole numbers  $x$  and  $y$  of ethanol and hydrogen reacting in reactions (1) and (2) respectively, the demand of heat of the reformer was then

calculated as:

$$\Delta H^{\text{ref}} = 173356x + 41166y \text{ J} \quad (10)$$

Similarly, when  $z$  is the number of CO moles reacting in reaction (3), the heat release due to the CO-shift reaction was easily calculated as:

$$\Delta H^{\text{shift}} = -41166z \text{ J} \quad (11)$$

The calculation of the heat released from the CO-remover was straightforward given by the knowledge of the CO moles that are selectively burnt and the enthalpy difference of the CO oxidation reaction which is  $\Delta H^{\text{CO}} = -282964 \text{ J mol}^{-1}$ . Similarly, for the reactions in the PEMFC and the burner the heat of hydrogen oxidation was  $\Delta H^{\text{H}_2} = -248818 \text{ J mol}^{-1}$ . The heat transfer regime of the plant was controlled through two parameters, the factor  $h$  of heat release from the burner (taken usually equal to 80%) and the factor of heat release from all other devices (which was taken equal to 100% in all cases).

## 2.2. Exergy calculations

Every flow of matter (or heat) is capable of producing an amount of useful work due to its chemical, thermal or mechanical energy content that attain a non-zero value whenever the macroscopic properties of chemical potential, temperature or pressure respectively are in a departure from the corresponding values of the environment [12,13]. However, a given amount of energy does never convert completely into useful work due to entropy generation. The useful part of energy, the so-called “exergy”, has been widely accepted as a measure of the quality or usefulness of the energy amount and “exergy analysis” has been regarded as the most rational method for the evaluation of the performance of the energy systems. Exergy may be considered as the sum of two components: physical and chemical exergy. Physical exergy is the useful work that a substance can produce when brought reversibly from its state to the “restricted dead state”, i.e. in a state of thermal and mechanical equilibrium with the environment. This postulation clearly shows that exergy is a property depending on both the state of the substance and the state of environment. By defining the temperature and the pressure of the environment as  $T_0 = 298.15 \text{ K}$  and  $p_0 = 1.013 \text{ bar}$  respectively, the physical exergy component  $e_i^{\text{PH}}$  of a substance  $i$  at temperature  $T$  and pressure  $p$  is given by:

$$e_i^{\text{PH}} = (h - h_0)_i - T_0(s - s_0)_i \quad (12)$$

where  $h_0$  and  $s_0$  denote the specific enthalpy and entropy evaluated at standard conditions, respectively.

Chemical exergy is the useful work that a substance can produce when it is brought reversibly from the “restricted dead state” to “dead state”, i.e. in a state of thermal, mechanical and chemical equilibrium with the environment. For the estimation of the chemical exergy component  $e_i^{\text{CH}}$  it is essential that the chemical species comprising the system should

Table 2

The environmental composition and the standard chemical exergy of every chemical species involved in the study

Chemical species	Environmental composition (vol.%)	Standard chemical exergy ( $\text{J mol}^{-1}$ )
N <sub>2</sub>	75.60	720
O <sub>2</sub>	20.34	3970
H <sub>2</sub> O(g)	3.12	9500
CO <sub>2</sub>	0.03	19870
Ar	0.91	11690
C <sub>2</sub> H <sub>6</sub> O		1357700
CO		275100
H <sub>2</sub>		236100
Total	100%	

be referred to the properties of a suitable selected set of environmental substances. Accordingly, an appropriate “exergy reference environment” is usually used in order to estimate the standard chemical exergy  $e_i^{\text{CH}}$  according to the relation

$$e_i^{\text{CH}} = -RT_0 \ln x_i^e \quad (13)$$

where  $x_i^e$  is the molar fraction of the species  $i$  in the standard reference environment. For compounds that do not form the environmental composition, the chemical exergy is estimated according to a standard procedure described elsewhere [12,13,21]. Table 2 presents the environmental composition which was assumed in the present work together with the values of the standard chemical exergy of all the species that were encountered in the analysis.

Finally, for a heat flow  $Q_i$  from a hot sink of temperature  $T_H$ , the exergy is simply equal to the reversible work that this can produce in an ideal Carnot cycle operating between the temperature limits of  $T_H$  and  $T_0$ . Therefore, the exergy of the heat flow  $Q_i$  will be

$$e_i^{\text{heat}} = Q_i(1 - T_0 T_H^{-1}) \quad (14)$$

## 3. Results and discussion

### 3.1. Avoidable PEMFC exergy destruction due to voltage adjustment

Fig. 1 illustrates the operation conditions of the power system together with the exergy flows in each stream of matter and heat. The conditions selected were  $T_{\text{ref}} = 600 \text{ K}$ ,  $T_{\text{shift}} = 400 \text{ K}$ ,  $T_{\text{cell}} = 400 \text{ K}$ ,  $\text{RF} = 3$ ,  $\lambda = 3$ ,  $U = 70\%$  and  $V = 0.5 \text{ V}$ . The extents of the reactions inside the reformer (1) and (2) as well as the CO-shift reaction are calculated equal to 92.86%, 18.85% and 92.86%, respectively. The molar compositions in each stream of matter in the system shown in Fig. 1 are provided in Table 3. In every device of the plant, the exergy balance provides an amount of exergy destruction, which for all actual processes has to be of a positive value. Negative exergy destruction in one or more individual subsystems of the plant implies a violation of the second law and an operation regime which is unfeasible in practice.



Table 3

The compositions of the streams of matter in the system shown of Fig. 1 in molar fractions (%)

Flow	Ethanol	H <sub>2</sub> O	CO <sub>2</sub>	H <sub>2</sub>	CO	O <sub>2</sub>	N <sub>2</sub>	Ar	Total
1	100.00	0.00	0.00	0.00	0.00	0.00	0.00	0.00	100.00
2	0.00	100.00	0.00	0.00	0.00	0.00	0.00	0.00	100.00
3	25.00	75.00	0.00	0.00	0.00	0.00	0.00	0.00	100.00
4	0.93	8.04	18.81	66.96	5.26	0.00	0.00	0.00	100.00
5	0.93	3.15	23.70	71.85	0.38	0.00	0.00	0.00	100.00
6	0.92	3.16	23.90	71.32	0.00	0.00	0.69	0.01	100.00
7	0.00	3.12	0.03	0.00	0.00	20.34	75.60	0.91	100.00
8	0.00	15.96	0.02	0.00	0.00	11.33	72.17	0.53	100.00
9	1.83	6.31	47.73	42.73	0.00	0.00	1.38	0.02	100.00
10	0.00	3.12	0.03	0.00	0.00	20.34	75.60	0.91	100.00
11	0.00	27.60	24.20	0.00	0.00	0.00	47.63	0.57	100.00

Under the conditions of Fig. 1, the exergy destruction in the vaporizer/mixer is equal to 11.60% of the chemical exergy of ethanol. This value is expected to remain unchanged when the plant operates with constant values of ethanol mass flow (in  $\text{kg s}^{-1}$ ), reforming factor RF, and vaporization temperature. Indeed, this value is the exergy destruction associated with the phase changes of ethanol and water (from  $T_0$  to  $T = 373.15$  K) and the mixing process of the gaseous products of the vaporization. The exergy balance takes into account the exergy of the incoming (liquid ethanol and liquid water acquire only chemical exergy given that they are taken at the restricted dead state) and outgoing streams of matter, and the exergy of the heat flowing to the vaporizer from the burner.

Similarly, the exergy balance of the reformer indicates an exergy destruction rate equal to 0.26 due to chemical reactions (1) and (2) at the respective extents. The exergy destruction rate of the CO-shift reactor is only 0.16 due to the low extent of the shift reaction. The amount of CO leaving the CO-shift reactor is burned stoichiometrically in the CO-remover inducing an exergy destruction of 0.39. Finally, the CO-free mixture of hydrogen (71.32% in molar basis) is routed to the PEMFC anode. The residual ethanol amount (0.92% in molar basis) is considered unaffected by the anode environment due to the low operating temperature of the PEMFC. Therefore, in the PEMFC the only reaction that occurs is the electrochemical oxidation of a percentage ( $U = 70\%$ ) of the hydrogen of the feed-stream, according to reaction (5). The products of this reaction are steam (in the cathode), electricity (equal to 27.22% of the chemical exergy of ethanol) and heat which is assumed to reject in the cooling media of the cell. The overall exergy destruction rate in the PEMFC is calculated by the exergy balance equal to 20.44%. Finally, the hydrogen amount which remains unreacted from the PEMFC and the amount of the residual ethanol undergo a stoichiometric combustion process in the burner that provide the heat to sustain the processes of vaporization and reforming. The heat rejected from the burner was assumed to have an efficiency of 80% with the rest 20% being absorbed by the combustion products. In Fig. 1, the exergy destruction in the burner is 13.73%. This value is characteristic of the irreversibility of the combustion processes of hydrogen and ethanol and is unchanged unless

the amounts of the reactants, the temperature of the burner or the stoichiometry of the combustion is changed.

The overall exergy destruction in the operation regime of Fig. 1 is 46.58% and the electrical efficiency of the plant is 27.22%. From the 46.58 units of total exergy destruction (ED), 43.88% is due to the irreversibility in the PEMFC, another 24.9% is due to the highly irreversible phase changes and mixing processes in the vaporizer and about 29.47% is due to 'combustion processes in the burner. When the cell voltage is increased from 0.5 to 0.6 V and 0.7 V, only the exergy destruction rate of the PEMFC is affected and lowers from 20.44% to 15.00% and 9.56%, respectively, providing an increase of the second law efficiency (here, the second law efficiency is considered as the ratio of the electrical work produced by the PEMFC to the standard chemical exergy of the ethanol input to the plant) to the corresponding values of 32.66% and 38.1%. A further increase of the cell voltage to 0.8 V would reduce the exergy destruction in the PEMFC to 4.11% with the exergy efficiency being 43.55%. This analysis illustrates that the exergy destruction in the PEMFC device is avoidable and subject to the appropriate adjustment of the cell voltage. On the other hand, the exergy destruction in the burner remains constant and subject to the overall thermal management of the plant. In principle, a well-designed plant of an automobile PEMFC system must operate with major exergy destruction rates in devices away from the energy output (electricity) and it is inevitable to have a significant exergy destruction in the vaporizer and the burner that undertakes the extremely irreversible combustion processes.

The effect of the cell voltage on the exergy destruction rate inside the PEMFC and the overall exergy efficiency of the cell system is presented in Fig. 2 in the voltage range of 0–0.9 V. As shown, the value of about 0.875 V is the maximum possible for the cell operation, above which the exergy destruction in the PEMFC becomes negative. Further, it is indicated that the maximum second law efficiency of the plant (at the conditions of  $T_{\text{ref}}$ ,  $T_{\text{shift}}$ ,  $T_{\text{cell}}$ ,  $\lambda$  and  $U$  of Fig. 1) is about 47.63%. This is the maximum attainable efficiency value but in practice the system is well controlled when the exergy destruction rate in the PEMFC has a low positive value of about 1–5%.

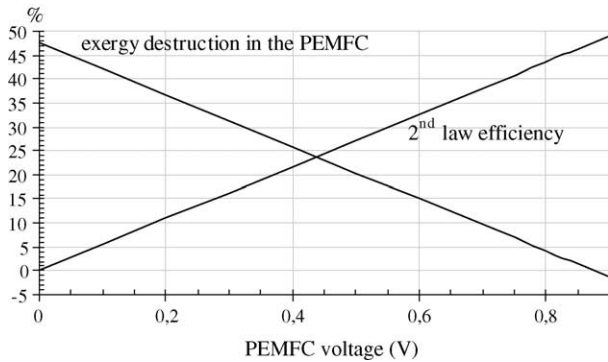


Fig. 2. The second law efficiency of the system and the exergy destruction rate in the PEMFC as a function of the PEMFC voltage at the operation conditions of Fig. 1.

### 3.2. Avoidable exergy loss and exergy destruction from the burner

It is important to notice that the operation of the plant does not present only exergy destructions but also exergy losses. For example, in the configuration of Fig. 1, a significant amount of exergy (6.74%) is lost away in the combustion products of the burner, while significant exergy losses are also due to heat wastes from all devices (except the vaporizer) to environment. In the case of the automobile engine examined in the present study, the exergy losses due to heat wastes from the reformer, the CO-shift reactor, the CO-remover and the PEMFC subsystems are unavoidable when desiring the PEMFC to operate at a practically rational temperature (at about 350–400 K). On the other hand, the desired thermal management of the system is highly responsible for the high exergy loss within the combustion products. However, the exergy loss due to heat released from the burner to environment is subject to the control of the designer. The heat released from the burner must be slightly higher than the heat demands of the vaporization and reforming processes and this may be controlled by an adjustment of the hydrogen utilization factor in the PEMFC. In the cases examined earlier, the hydrogen utilization factor was selected equal to  $U = 70\%$  in order to minimize the exergy loss from the burner to environment (0.44% in all previous cases). A further increase of the  $U$  value would result in a negative burner balance which would force the reformer and the vaporizer to operate at non-prescribed conditions. In contrast to exergy destructions due to entropy generating irreversibilities, exergy losses may be considered exploitable for practical applications according to the requirements of the designer (for cabin heating or other engineering purposes).

The burner balance may be expressed by the following general expression that provides the factor of hydrogen utilization  $U$  (%) as a function of the reforming factor, the extents and heats of the reactions (1)–(3), the heat of vaporization of ethanol and water at 373.15 K and the energy loss from the burner to environment  $l$  (as percentage of the LHV of the

ethanol inflow),

$$U = 413.534(-59792.54 - 12350l - 48169.8RF + 12350h(1 - x) - 173563x - 41166y + 2418.18h(6x - y + z))/(10^6h(6x - y + z)) \quad (15)$$

where  $h$  (%) is the heating efficiency of the burner (80% in the previous cases) and  $x$ ,  $y$  and  $z$  are the moles reacting in reactions (1), (2) and (3). Eq. (15) is valuable in estimating the factor of hydrogen utilization from the energy balance of the burner as shown in Fig. 3a. With the conditions from the vaporizer up to the CO-remover being identical with those of Fig. 1, and with the cell operating at  $V = 0.8$  V, Fig. 3a illustrates the effect of the energy loss from the burner to environment on the factor of hydrogen utilization,  $U$ , on the second law efficiency of the plant and on the total amounts of exergy destruction and exergy losses. As shown, the zero-loss burner balance requires a hydrogen utilization of about 70.93%. In this case, the exergy (second law) efficiency of the plant (at  $V = 0.8$  V and  $h = 80\%$ ) is 44.12%, the total exergy destruction is  $ED = 29.96\%$ , the total exergy loss due to waste heat is  $ELH = 19.24\%$  and the exergy loss in the form of physical and chemical exergy of the flue gases is  $EFG = 6.62\%$ . Deviating from the zero-loss burner balance, the required factors of hydrogen utilization ought to be lower. For example, when the energy loss of the burner is  $l = 10\%$  of

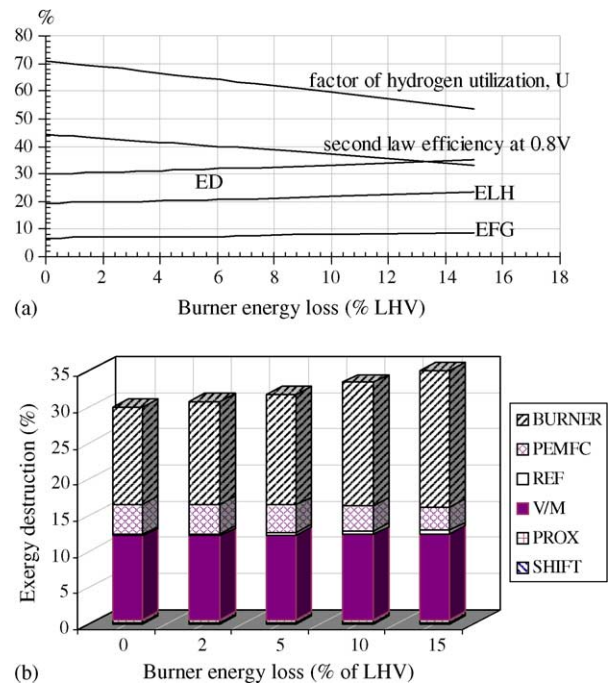


Fig. 3. (a) Effect of the burner balance on (i) the factor of hydrogen utilization,  $U$ , (ii) the total exergy destruction in the devices of the plant, ED, (iii) the total exergy loss due to rejection of heat to the environment, ELH and (vi) on the exergy loss within the flue gases, EFG ( $V = 0.8$  V; all other conditions are identical with that of Fig. 1). (b) Allocation of the exergy destruction in the devices of the power system at different conditions of burner balance ( $V = 0.8$  V and  $U$  changes according to (a)). All other conditions are identical with that of Fig. 1).

the LHV (i.e. 123,500 J) it is  $U = 59.41\%$ . At these conditions the second low efficiency is only 36.96% while both the total exergy destruction and losses increase. Fig. 3a illustrates that the prolonged deviation from the zero-loss burner regime induces additional exergy destruction and exergy losses, which should be avoided in the practical design. The higher is the heat waste from the burner the lower will be the efficiency of the plant, the higher will be the overall exergy destruction rate and the higher will also be the exergy losses.

The effect described above is illustrated also in Fig. 3b which allocates the exergy destruction rate in the individual subsystems of the plant for selected regimes of burner balance. As shown, at the zero-loss burner balance the overall exergy destruction rate is 29.96%. This is allocated with the percentages of 11.57% in the vaporizer, 0.25% in the reformer, 0.16% in the CO-shift reactor, 0.39% in the CO-remover, 4.17% in the PEMFC and 13.43% in the burner, respectively. Increasing the energy loss from the burner, the ex-

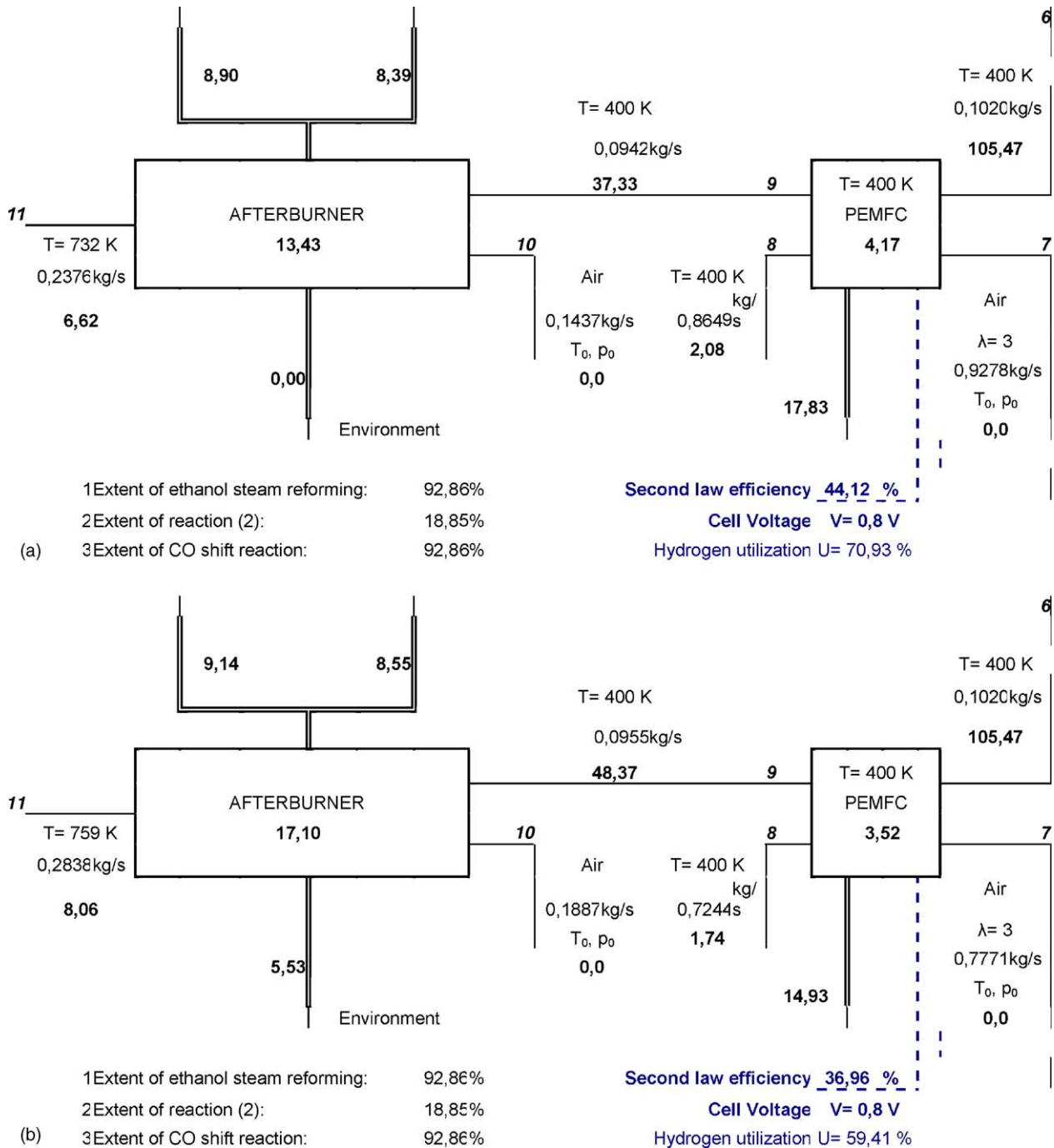


Fig. 4. Comparison of two operation configurations with 0% (a) and 10% (b) energy losses from the burner to the environment.



ergy destruction rate of the vaporizer increases from 11.57% at zero-loss conditions to about 11.91% at 15% losses. In the same range, the destruction rate of the reformer increases also from 0.25% to about 0.48%, the exergy destructions of the CO-shift and the CO-remover reactors remain constant and the exergy destruction in the PEMFC decreases from 4.17% to about 3.19%. However, all the aforementioned changes are small in comparison to the increase of the exergy destruction of the burner. By changing the burner balance from the zero-loss regime to a configuration of 15% loss, the exergy destruction in the burner increases from the value of 13.43% to about 18.85%. This increase of the exergy destruction of the burner is mostly responsible for the increase of the total exergy destruction of the overall power system. This effect may be clarified in detail in Fig. 4 where a comparison is made of the burner configurations with 0% and 10% energy losses.

### 3.3. Avoidable exergy destruction due to vaporization issues

As it is shown in Table 1, the reaction of ethanol reforming is favored for completion by high reforming factors. At  $T_{\text{ref}} = 600$  K, for example, the extent of the reaction (1) for  $\text{RF} = 3$  is 92.86% and for  $\text{RF} = 5$  about 99.99%. Further, assuming the reaction (2) and the reaction of the CO-shift reactor at  $T_{\text{shift}} = 400$  K, the number of  $\text{H}_2$  moles in the PEMFC feed-stream in the first case is about 5.54 and in the second 5.99 (assuming an ethanol feed-stream of  $1 \text{ mol s}^{-1}$ ). Based on this, one could consider that the increase of the reforming factor is capable of improving the performance of the PEMFC system, but this is not true. The demand for high reforming factors increases the heating demand of the vaporizer and despite of the increase of the hydrogen amount reaching the PEMFC it forces the system to operate at lower hydrogen utilization factors as it is predicted by Eq. (15). Indeed, as shown in Fig. 5, the selection of excess steam results in a lowering of the hydrogen utilization factor in a way similar to the reduction induced by the increase of the burner losses. However, as one may observe the distance between the curves of  $U$  for  $\text{RF} = 3$  and 4 is higher than that between the curves for  $\text{RF} = 4$  and 5 because of the relativity of the measure of

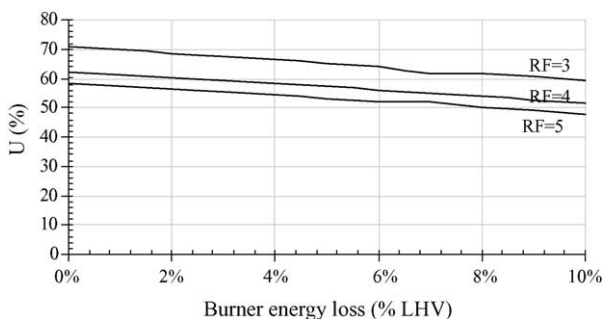


Fig. 5. Effect of the burner balance and the reforming factor, RF, on the value of the factor of hydrogen utilization,  $U$ .

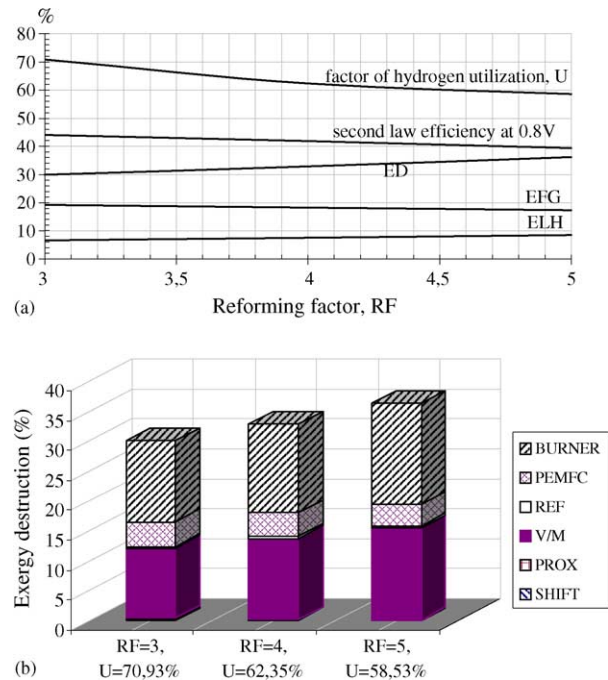


Fig. 6. (a) Effect of the reforming factor on (i) the factor of hydrogen utilization,  $U$ , (ii) the total exergy destruction in the devices of the plant, ED, (iii) the total exergy loss due to rejection of heat to the environment, ELH and (vi) on the exergy loss within the flue gases, EFG ( $V = 0.8$  V; all conditions refer at zero-loss burner balance with the rest independent variables being identical to that of Fig. 1). (b) Allocation of the exergy destruction in the devices of the power system at different conditions of burner balance ( $V = 0.8$  V and  $U$  changes according to (a)). All conditions refer at zero-loss burner balance with the rest independent variables being identical to that of Fig. 1).

the factor of hydrogen utilization which is a percentage of different amounts of hydrogen incoming the PEMFC at each RF regime.

Fig. 6a illustrates the effect of the reforming factor on the factor of hydrogen utilization, on the second law efficiency and on the total exergy destructions and losses ED, ELH and EFG for a plant operating at  $V = 0.8$  V and under conditions of zero-loss burner balance. As shown, the increase of the reforming factor results in a decrease of the factor  $U$  and lowers the overall exergy efficiency of the system from 44.12% at  $\text{RF} = 3$  to 39.38% at  $\text{RF} = 5$ . In terms of exergy, the utilization of excess steam provides a slight decrease of the value of EFG but, most importantly, it has the consequence of a dramatic increase of the overall exergy destruction in the plant (from  $\text{ED} = 29.96\%$  at  $\text{RF} = 3$  to about 36.24% at  $\text{RF} = 5$ ). Under the same conditions and at  $\text{RF} = 3, 4$  and 5, respectively, the allocation of the exergy destruction in the subsystems of the plant is shown in Fig. 6b. The exergy destruction rates that decrease with the utilization of excess steam are those inside the devices of the PEMFC (from 4.17% at  $\text{RF} = 3$  to 3.59% at  $\text{RF} = 5$ ), the CO-shift reactor (from 0.16% at  $\text{RF} = 3$  to 0.08% at  $\text{RF} = 5$ ) and the PROX reactor (from 0.39% at  $\text{RF} = 3$  to 0.06% at  $\text{RF} = 5$ ). However, the increase of the exergy destruction rate in the other devices is of a much higher mag-

nitude. In the vaporizer the exergy destruction rate increases from 11.57% at  $RF=3$  to about 15.36% at  $RF=5$ , while in the same  $RF$  range the destruction rates in the burner increase from 13.43% to 16.83%. On the whole, the utilization of excess steam is found to be of negative impact as it results in the addition of about 3 units of avoidable exergy destruction per each unit increment of the  $RF$ . This avoidable exergy destruction is essential to be minimized in practical applications by selecting  $RF$  values close to the stoichiometric value of  $RF=3$ . However, in practice it is generally preferred to use an excess of steam in the reforming reaction to force the reaction in completion and to avoid technical problems such as the formation of solid carbon in the reformer. The designer must be aware of these technical aspects so as to compromise the efficiency and the technical safety of the plant.

### 3.4. Effect of the reformer temperature

The temperature of the reformer is a crucial parameter in the design of the power plant since it has a direct effect on the extents of the reactions (1) and (2) that provide the hydrogen source of the PEMFC. Fig. 7a illustrates the effect of the reforming temperature in the range of 400–800 K assuming that the shift reactor operates constantly at 400 K and

the reforming factor is equal to  $RF=3$ . For a given reforming temperature, the extents of the reactions (1) and (2) are calculated and Eq. (15) is used to determine the hydrogen utilization factor on a zero-loss burner condition basis (i.e.  $l=0$ ). For  $T_{ref}=400$  K, the energy balance of Eq. (15) predicts a factor of hydrogen utilization above 100%, indicating that the zero-loss burner balance is impossible at these conditions. Indeed, in this regime the extent of the reforming reaction (1) is only 21.99% (see Table 1) and even the 100% utilization of hydrogen in the PEMFC induces the tremendous loss of the 42.7% of the LHV of the ethanol input of the plant in the form of heat loss from the burner to the environment. Due to this, the exergy destruction in the burner, the overall exergy loss due to heat rejection ELH and the overall exergy destruction ED are extremely high (32.05%, 29.57% and 45.66%, respectively) and the exergy efficiency of the plant has the unacceptable low value of about 14.81%. At  $T_{ref}=500$  K, the extent of the reforming reaction increases to about 69.08% and the zero-loss burner regime is now feasible for  $U=97.45\%$ . In this regime, the values of ED, ELH and EFG are passing through a minimum (29.81%, 18.81% and 6.00%, respectively) and the value of the exergy efficiency of the plant attains a maximum of 45.29%. Further increase of the reforming temperature above 500 K increases the values of ED, ELH and EFG with an overall consequence the lowering of the exergy efficiency of the plant from 45.29% at 500 K to about 42.07% at 800 K (with the PEMFC operating always at 0.8 V).

The allocation of exergy destructions in the devices of the plant, is given in Fig. 7b for five scenarios of reforming temperatures in the range of 400–800 K. At the worse scenario of  $T_{ref}=T_{shift}=400$  K, the shift reactor is useless and has a zero exergy destruction, while about 71% of the overall ED occurs in the burner. In this case the current drawn is extremely low and the plant operates more like an ethanol burner. At  $T_{ref}=500$  K the exergy destruction rates in the devices of the plant are as follows: vaporizer 11.24%, reformer 0.47%, shift reactor 0.01%, PROX 0.06%, PEMFC 3.94% and burner 14.09%. Finally, at higher reforming temperatures the exergy destruction rates of all devices except the vaporizer and the reformer tend to increase in comparison with their corresponding values at about 500 K. This analysis shows that the selection of the reforming temperature at  $T_{ref}=500$  K is the best choice among the examined scenarios.

### 3.5. Effect of the temperature of the shift reactor

By considering the temperature of the reformer constant and the plant operating with  $RF=3$  and  $h=80\%$ , in a standard loss burner regime (for example at  $l=0$ ), it is useful to examine the effect of the temperature of the shift reactor on the performance of the plant, given that this is also an independent variable selected a priori by the designer. Since the shift reaction (3) is exactly the opposite of reaction (2) which takes place in the reformer, it is evident that the temperature of the shift reformer must always be lower than that of the

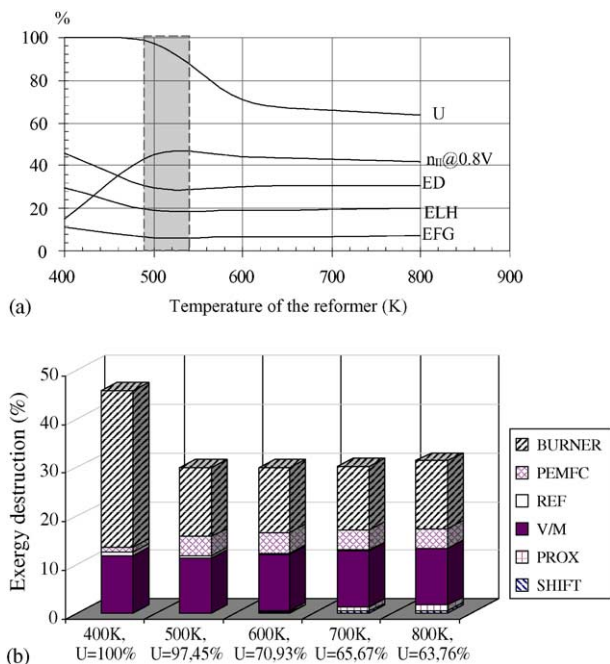


Fig. 7. (a) Effect of the temperature of the reformer on the factor of hydrogen utilization  $U$ , on the second law efficiency of the plant and on the ED, ELH and EFG amounts for the plant operating at  $V=0.8$  V with  $RF=3$ . (The temperature of the shift reactor is kept at 400 K and all conditions refer to zero-loss burner balance. The highlighted region is the most appropriate for operation.) (b) Allocation of the exergy destruction in the devices of the power system at different temperatures of the reformer reactor ( $V=0.8$  V and  $U$  changes according to (a)). All conditions refer at zero-loss burner balance except the case for  $T_{ref}=400$  K which corresponds to heat loss from the burner equal to of 42.7% of the LHV of ethanol. The shift reactor was kept to operate at 400 K).

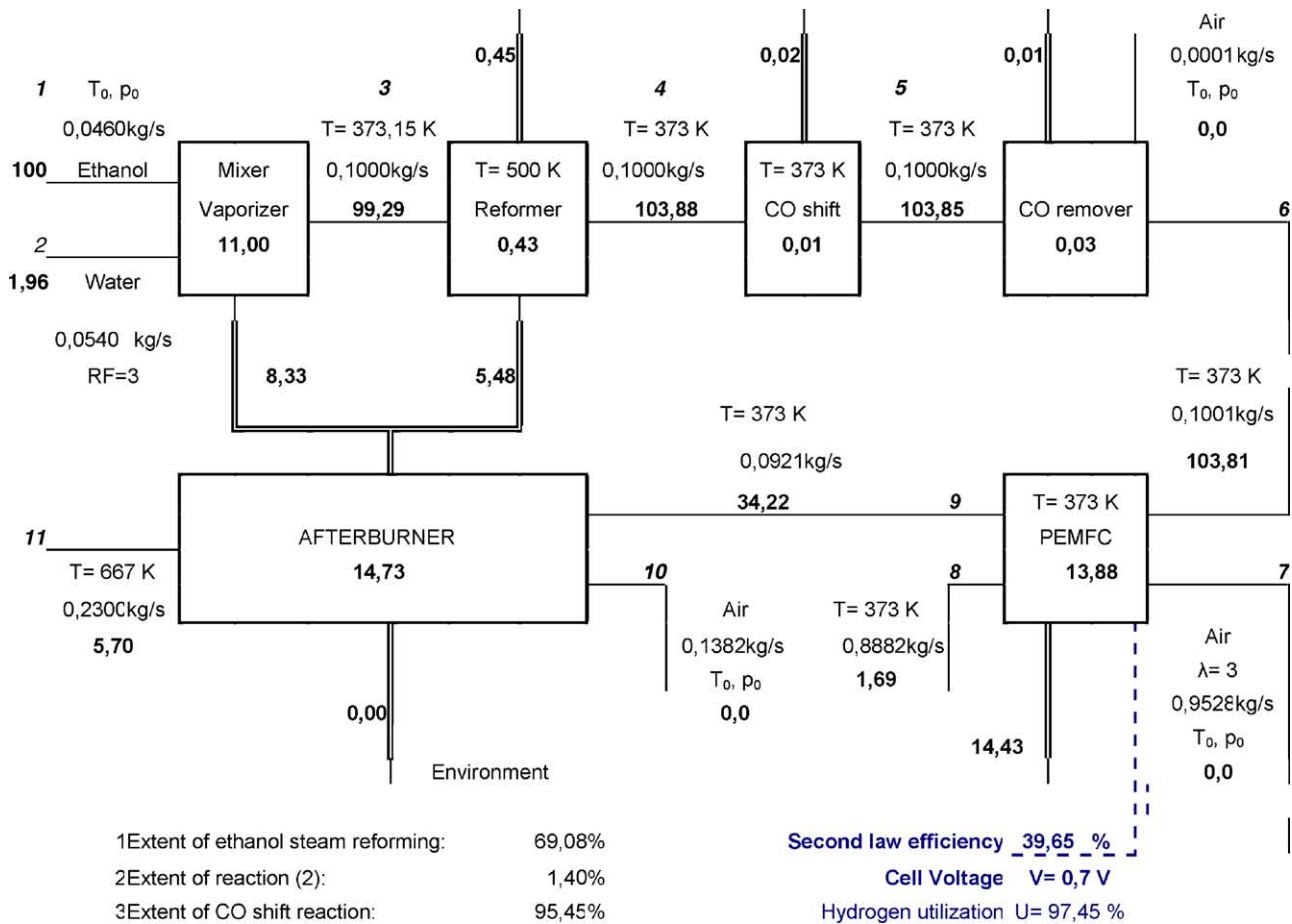


Fig. 8. Analysis of the PEMFC power system for  $T_{ref} = 500\text{ K}$ ,  $T_{shift} = 373.15\text{ K}$ ,  $U = 97.45\%$ ,  $V = 0.7\text{ V}$ . The second law efficiency is 39.65%. Even higher efficiencies are attainable at higher voltages since the exergy destruction in the PEMFC is rather high.

reformer. Thus, assuming  $T_{ref} = 600\text{ K}$  and  $T_{shift} = 400\text{ K}$ , the regime of the plant is that of Fig. 1 and the maximum possible voltage output derived in Fig. 2 was equal to about 0.875 V (second law efficiency about 48.26% at zero-loss burner conditions). The shift reaction is slightly exothermic and therefore it is favored at lower temperatures. In this respect it is expected that the lowering of the shift reactor temperature

will be beneficial for the plant performance. Indeed, at the lowest feasible temperature  $T_{shift} = 373.15\text{ K}$  (below which steam condensation problems arise) the extent of the shift reaction is higher than that of Fig. 1 and Eq. (15) predicts a hydrogen utilization factor  $U = 71.01\%$  for  $l = 0$ . In this case an analysis analogous to that of Fig. 2 may show that the PEMFC device has a higher exergy input and thus may oper-

Table 4  
The compositions of the streams of matter in the system of Fig. 8 in molar fractions (%)

Flow	Ethanol	H <sub>2</sub> O	CO <sub>2</sub>	H <sub>2</sub>	CO	O <sub>2</sub>	N <sub>2</sub>	Ar	Total
1	100.00	0.00	0.00	0.00	0.00	0.00	0.00	0.00	100.00
2	0.00	100.00	0.00	0.00	0.00	0.00	0.00	0.00	100.00
3	25.00	75.00	0.00	0.00	0.00	0.00	0.00	0.00	100.00
4	4.57	14.31	19.83	60.69	0.60	0.00	0.00	0.00	100.00
5	4.57	13.74	20.40	61.26	0.03	0.00	0.00	0.00	100.00
6	4.57	13.74	20.42	61.22	0.00	0.00	0.05	0.00	100.00
7	0.00	3.12	0.03	0.00	0.00	20.34	75.60	0.91	100.00
8	0.00	15.96	0.02	0.00	0.00	11.33	72.17	0.53	100.00
9	11.33	34.06	50.62	3.87	0.00	0.00	0.13	0.00	100.00
10	0.00	3.12	0.03	0.00	0.00	20.34	75.60	0.91	100.00
11	0.00	27.07	25.64	0.00	0.00	0.00	46.73	0.56	100.00

ate at higher voltage, specifically up to  $V=0.95$  V providing an exergy efficiency of 52.6%. This slight decrease of the temperature of the shift reactor from 400 to 373.15 K has as a major consequence on a better thermal management of the plant and a drop of the exergy losses due to heat rejection to the environment. By comparing both plants at their maximum voltage with  $RF=3$ ,  $h=80\%$ ,  $l=0$  and  $T_{ref}=600$  K, the plant with  $T_{shift}=400$  K is characterized by the amounts  $ED=21.82$ ,  $ELH=19.24$ ,  $EFG=6.63$  while the respective values for the plant with  $T_{shift}=373.15$  K are  $ED=26.21$ ,  $ELH=15.27$  and  $EFG=6.30$ . Moreover, by reminding the analysis of the previous section and the conclusions for the effect of the temperature of the reformer, a decrease of the  $T_{ref}$  at 500 K when  $T_{shift}=373.15$  K is expected to further improve the plant performance. In detail, in this regime Eq. (15) provides a factor  $U=97.45\%$  for  $l=0$  and the new efficiency is even higher. At the practically reasonable voltage of 0.7 V the second law efficiency is approximately 39.65%. The configuration of the plant in this case is given in Fig. 8 and the information of the composition of each stream of matter in this system is shown in Table 4.

#### 4. Conclusions

The results presented in the present work provide a systematic analysis of an automobile PEMFC power unit utilizing first and especially second law considerations. A typical automobile PEMFC power plant with external steam reforming and the necessary auxiliary equipment was contemplated being powered by liquid ethanol. The exergy analysis method was used and design guidelines were clarified for the most crucial operating parameters such as the PEMFC output, the burner balance, the selected reforming factor and the temperatures of the reformer and CO-shift reactors. The underlying concept for every design decision was the adjustment of the operating parameters to avoid unnecessary exergy destruction or exergy loss and a detailed explanation of these interactions was provided. The major conclusions of this work are summarized as follows:

- Exergy destruction in the PEMFC device is the most crucial parameter for elimination. In every operation regime, the cell voltage must be appropriately adjusted so as to fully exploit the exergy amount remaining in the PEMFC subsystem. In each case, the plant efficiency maximization corresponds exactly at the conditions of maximum cell voltage – minimum cell exergy destruction.
- Maximization of the hydrogen utilization for electricity generation requires a direct minimization of the exergy loss from the secondary power unit of the plant—the burner. The governing relationship of the overall energy balance of the plant was derived to facilitate calculations in this specific direction. As it was indicated, the burner balance is crucial for the control of the overall exergy construc-

tion and exergy loss, allowing the convergence to a single optimal design (zero-loss burner balance).

- Avoidable exergy destruction due to vaporization issues was allocated in the plant and allowed for the recognition of the role of the reforming factor in its performance. As a concluding rule, it was demonstrated that the utilization of excess steam results in an increase of the overall exergy destruction providing a concomitant lowering to the plant efficiency. An appropriately high value of RF for carbon-free PEMFC operation is necessary and a compromise with a slight efficiency deterioration is inevitable in practice.
- The overall effect of the temperature of the reformer reactor was clarified and allowed for the recognition of the best region for the specific application. In the same direction, the appropriate conceptual background for the selection of the temperature of the shift reactor has been also presented with emphasis on the combinatorial role of these two temperature parameters in the performance of the plant. The interactions that these parameters induce on the exergy flow chart of the plant was discussed.

#### Acknowledgement

The authors gratefully acknowledge financial support by the “*Pythagoras 2004 EPEAEK B*” programme from the Greek Ministry of National Education and Religious Affairs.

#### References

- [1] S.L. Douvartzides, F.A. Coutelieris, A.K. Demin, P.E. Tsiakaras, Int. J. Hydrogen Energy 29 (2004) 375.
- [2] M.K. Evans, The economic impact of the demand for ethanol, prepared for the Midwestern Governor’s Conference, Lombard, IL, USA, 1997.
- [3] J. Ramírez-Salgado, A. Estrada-Martínez, J. Power Sources 129 (2) (2004) 255.
- [4] L.B. Lave, W.M. Griffin, H.L. MacLean, Issues Sci. Technol. 18 (2) (2002) 73.
- [5] A.E. Comyns, Focus Catal. (4) (2004) 1.
- [6] G.A. Deluga, J.R. Salge, L.D. Schmidt, X.E. Verykios, Science 303 (2004) 993.
- [7] J. Sun, X. Qiu, F. Wu, W. Zhu, W. Wang, S. Hao, Int. J. Hydrogen Energy 29 (10) (2004) 1075.
- [8] H.L. MacLean, L.B. Lave, Prog. Energy Combust. Sci. 29 (1) (2003) 1.
- [9] V. Klouz, V. Fierro, P. Denton, H. Katz, J.P. Lisse, S. Bouvot-Mauduit, C. Mirodatos, J. Power Sources 105 (1) (2002) 26.
- [10] F.R. Kalhammer, Status and Prospects of Fuel Cells as Automobile Engines, Fuel Cell Technical Advisory Panel, Sacramento, CA, USA, 1998.
- [11] K. Kordesch, G. Simader, Fuel Cells and their Applications, VCH Verlagsgesellschaft, Weinheim, Germany, 1997.
- [12] T.J. Kotas, The Exergy Method of Thermal Plant Analysis, Butterworths, London, 1985.
- [13] A. Bejan, G. Tsatsaronis, M. Moran, Thermal Design and Optimization, Wiley, 1996.
- [14] M.A. Rosen, Int. J. Energy Res. 23 (5) (1999) 415.
- [15] P.F. van der Oosterkamp, A.A. Goorse, L.J. Blomen, J. Power Sources 41 (1993) 239.



- [16] R. Cownden, M. Nahon, M.A. Rosen, *Exergy Int. J.* 1 (2) (2001) 112.
- [17] A. Ishihara, S. Mitsushima, N. Kamiya, K. Ota, *J. Power Sources* 126 (2004) 34.
- [18] A. Kazim, *Energy Convers. Manage.* 45 (2004) 1949.
- [19] J. Larminie, A. Dicks, *Fuel Cell Systems Explained*, Wiley, 2001.
- [20] V. Majer, V. Svodoba, *Enthalpies of Vaporization of Organic Compounds: A Critical Review and Data Compilation*, Blackwell Scientific Publications, Oxford, 1985.
- [21] J. Szargut, D.R. Morris, F.R. Steward, *Exergy Analysis of Thermal, Chemical and Metallurgical Processes*, Hemisphere, New York, 1988, pp. 297–309.